Available online at www.sciencedirect.com
ScienceDirect
Nuclear Physics B (Proc. Suppl.) 169 (2007) 371–378
NUCLEAR PHYSICS B PROCEEDINGS SUPPLEMENTS
www.elsevierphysics.com

Physics with Tau Leptons at HERA

C. Veelken[a] on behalf of the H1 and ZEUS collaborations

[a]Department of Physics, University of California,
One Shields Avenue, Davis, CA 95616

Recent results of analyses investigating the production of tau leptons in ep collisions at HERA are reviewed. In total, four different types of analyses are presented: the production of $\tau^+\tau^-$ pairs, the production of single, isolated tau leptons in events with large missing transverse momentum (in addition to that resulting from the tau decay); plus two searches for specific new phenomena - for doubly charged Higgs bosons with subsequent decay $H^{++} \to e^+\tau^+$ and for tau leptons produced in lepton flavor violating processes $ep \to \tau X$.

1. Introduction

Within the Standard Model (SM), tau leptons are expected to be only rarely observed at HERA. The dominant production mechanism, the production of $\tau^+\tau^-$ pairs in photon–photon collisions has a cross–section of about 20 pb to produce tau lepton with transverse momenta above 2 GeV [1]. The cross–section for the production of single tau leptons in events with large missing transverse momentum is even smaller, of the order 0.1 pb [2]. The observed rate of tau lepton production at HERA may, however, be significantly enhanced by contributions from new physics.

In this paper, studies of SM tau lepton production and searches for BSM phenomena producing tau leptons in the final state are presented, using data collected in ep collisions at HERA. The analyzed datasets were recorded by the H1 and ZEUS experiments in the years 1994–2006 and correspond to integrated luminosities of up to 341 pb^{-1} (H1) and 250 pb^{-1} (ZEUS).

2. Experimental Conditions

2.1. The HERA Collider

In the HERA storage ring, electrons [1] are accelerated to a beam energy of $E_e = 27.6$ GeV and protons to a beam energy of $E_p = 920$ GeV (since 1998; in the years 1994–97 HERA was operated with a proton beam energy of 820 GeV), yielding an ep center–of–mass energy of $\sqrt{s} = 318$ GeV (301 GeV in the period 1994–97).

2.2. The Experiments H1 and ZEUS

The H1 and ZEUS detectors are designed as general purpose detectors, similar in construction to particle detectors used at other high energy physics experiments.

In the center of both detectors, enclosing the nominal interaction point, silicon vertex detectors are installed. The silicon vertex detectors are complemented by planar and cylindrical drift chambers which provide tracking information up to higher radii. The transverse momenta of charged particles are measured by the curvature of tracks in a solenoidal magnetic field. Electromagnetic and hadronic calorimeters surround the tracking detectors. The iron return yokes of the solenoid magnets providing the magnetic fields in the tracking detectors are instrumented with limited streamer tubes for muon detection. For the detection of penetrating particles produced at small polar angles, separate forward muon detectors are installed behind the main H1 and ZEUS detectors in proton beam direction.

In both experiments, a right handed coordinate system is used, in which the z–axis is defined by the proton beam direction. The polar angles θ and transverse momenta P_T of particles produced in the ep interactions are defined with respect to

[1]The HERA collider can be operated with either electrons or positrons. In the following, the term "electron" will be used generically to describe either electrons or positrons unless specifically noted.

0920-5632/$ – see front matter
doi:10.1016/j.nuclphysbps.2007.03.027

the z–axis and the azimuthal angle ϕ defines the particle direction in the transverse plane. The pseudo–rapidity η is defined as $\eta = -\ln\tan\frac{\theta}{2}$.

A more detailed description of the H1 and ZEUS detectors can be found in [3] and [4], respectively.

3. Analyses of $\tau^+\tau^-$ Pair–Production

The analyses of $\tau^+\tau^-$ pair–production complements previous H1 [5, 6] and ZEUS analyses [7] of electron and muon pair–production. An H1 analysis of multi–electron production has found 3 tri–electron and 3 di–electron events with an invariant mass (of the highest P_T electron pair) above 100 GeV [5], a region where only 0.30 ± 0.04 and 0.23 ± 0.04 events are expected from SM processes [2]. It is therefore interesting to investigate if $\tau^+\tau^-$ pairs of high invariant mass or P_T are present in the H1 and ZEUS data.

3.1. H1 Analysis

In the H1 analysis, $\tau^+\tau^-$ events are selected in a combination of leptonic ($e + \mu$), semi–leptonic (e+jet, μ+jet) and hadronic (jet+jet) decay channels of the two tau leptons.

Electrons are identified by the presence of a compact isolated cluster in the electromagnetic calorimeter and are required to have an anergy above 5 GeV and to be within the angular range $20^\circ < \theta_e < 140^\circ$.

Muons are identified by associating an isolated track in either the planar or cylindrical drift chambers with a track segment or an energy deposit in the instrumented iron and are required to be within the angular range $20^\circ < \theta_\mu < 140^\circ$ and have a transverse momentum above 2 GeV.

Jets resulting from hadronic tau decays (denoted as "tau–jets" in the following) are identified by a set of neural networks trained to discriminate between hadronic one–prong and three–prong tau decays on the one hand and electrons, muons and jets resulting from hadronization of quarks and gluons ("hadronic jets") on the other hand. For the training of the neural networks, a set of jet–shape observables reconstructed from hits in the drift chambers and from energy deposits in the calorimeters are used [8]. The jets are required to contain at least one track with a transverse momentum $P_T^{track} > 2$ GeV and to be within the angular range $20^\circ < \theta_{jet} < 120^\circ$.

In order to reduce background contributions, the events are required to be compatible with elastic production, i.e. to contain neither energy deposits above noise level in the calorimeter nor tracks in the drift chambers that cannot be associated with either the tau decay products or the scattered electron.

In an $e^\pm p$ dataset corresponding to an integrated luminosity of 106 pb^{-1}, 30 events are selected in the combination of leptonic, semi–leptonic and hadronic decay channels. The number of events selected in the data is in agreement with a SM prediction of 27.1 ± 4.1 events, of which 59% are expected from $\tau^+\tau^-$ (signal) processes. The distribution of the transverse momenta of the visible decay products (e, μ or jet) is shown in figure 1. The P_T distribution as well as the distribution of the invariant mass of the detected decay products are found to be in agreement with the SM expectation [9].

In the kinematic region defined by $20^\circ < \theta_\tau < 140^\circ$ and $P_T^\tau > 2$ GeV, the measured cross–section is $13.6 \pm 4.4 \pm 3.7$ pb [9] (the first error represents statistical and the second systematic uncertainties), in agreement with a SM expectation of 11.2 ± 0.3 pb [1].

3.2. ZEUS Analysis

In the analysis performed by the ZEUS collaboration, $\tau^+\tau^-$ events are selected in the leptonic ($e + \mu$) decay channel only.

Electrons are required to have an energy $E_e > 4$ GeV and to be within the angular range $\theta_e < 2.6$ rad. For electrons within the geometric acceptance of the cylindrical drift chamber ($17^\circ < \theta < 164^\circ$), a track of momentum $P_{track} > 2$ GeV is required to match the electron cluster.

Muons are identified by a combination of their minimum ionizing particle signatures in the calorimeter and hits reconstructed in the muon detectors. They are required to match a track of $P_T^\mu > 2$ GeV in the cylindrical drift chamber.

[2] Here and in the following, uncertainties quoted on SM predictions represent systematic and statistical uncertainties added in quadrature, unless specifically indicated otherwise.

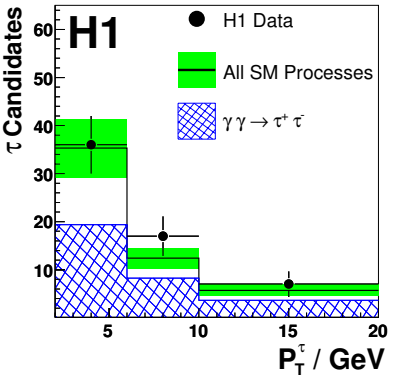

Figure 1. Distribution of transverse momenta of the visible tau decay products in the H1 $\tau^+\tau^-$ event sample. Note that selected events enter the distribution twice. The open histogram shows the SM expectation and the shaded band its uncertainty. The signal contribution is indicated by the hatched histogram.

As in the H1 analysis, the events are required to be compatible with elastic production, in order to reduce the contributions from various background processes.

In an e^-p dataset corresponding to an integrated luminosity of 135 pb^{-1}, 3 events are selected, in agreement with a SM expectation of 2.0 ± 0.8 events from $\tau^+\tau^-$ (signal) processes plus less than 0.2 from $\mu^+\mu^-$ (background) processes. The P_T and invariant mass distributions of the detected decay products are found to be in agreement with the SM prediction as well.

4. Analyses of events containing single tau leptons and large missing transverse momentum

The analysis of events containing single, isolated tau leptons and large missing transverse momentum (P_T^{miss}) is motivated by the observation of an excess over the SM expectation of events containing isolated electrons or muons and large P_T^{miss} in the H1 data [10]. Such events are produced by tauonic decays $W \to \tau\nu$ of real W bosons and can be a signature of physics beyond the SM, such as the anomalous production of single top quarks by flavor–changing neutral current interactions [11].

4.1. H1 Analysis

The H1 analysis of $\tau + P_T^{miss}$ events is based on the identification of the hadronic one–prong decay modes of the tau. One–prong tau–jets of $P_T^{jet} > 7$ GeV are identified within the angular range $20° < \theta_{jet} < 120°$ by requiring a jet of radius $R_{jet} < 0.12$ that contains exactly one track, which is required to have a transverse momentum $P_T^{track} > 5$ GeV. The jet radius R_{jet} is defined as the energy weighted average distance in η–ϕ between the jet–axis and all particles i within the jet:

$$R_{jet} = \frac{1}{E_{jet}} \sum_i E_i \sqrt{\Delta\eta\,(jet,i)^2 + \Delta\phi\,(jet,i)^2}\,.$$

The decay products of the tau lepton are excluded from the reconstruction of the hadronic final state X.

For events to be selected, a missing transverse momentum of $P_T^{miss} > 12$ GeV is required. In order to ensure that the reconstructed P_T^{miss} arises neither from a mismeasurement of the hadronic final state nor (solely) from the neutrino produced in the tau decay, an angle ("acoplanarity angle") $\left|\phi^{jet} - \phi^X\right| < 170°$ between the one–prong tau jet and the hadronic final state is required. A few further selection criteria are applied, to reduce remaining contributions of background processes [9, 12].

In an $e^\pm p$ dataset corresponding to an integrated luminosity of 278 pb^{-1}, 25 events are selected, in agreement with a SM expectation of $24.2^{+4.2}_{-5.8}$. As is illustrated in figure 2, a fluctuation over the SM prediction is observed at large hadronic transverse momenta, however. In the region $P_T^X > 25$ GeV, 3 events are observed, while only $0.74^{+0.19}_{-0.16}$ events are expected from all SM processes (the main contribution of which, $0.44^{+0.07}_{-0.09}$ events, is expected from tauonic decays $W \to \tau\nu$ of real W bosons).

4.2. ZEUS Analysis

The ZEUS $\tau + P_T^{miss}$ analysis is also based on identifying the hadronic one–prong tau decay modes.

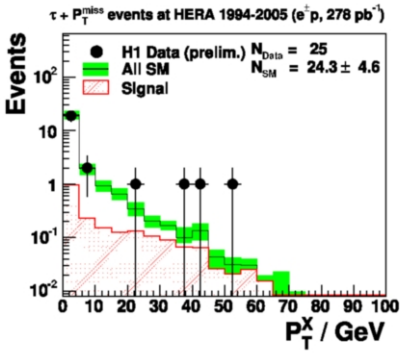

Figure 2. Distribution of the hadronic transverse momentum in the $\tau + P_T^{miss}$ events selected in the H1 $e^{\pm}p$ data (points), compared to the SM expectation (open histogram). The contribution from W boson decays is indicated by the hatched histogram.

Loose tau–jet candidates are selected within the angular range $-1.0 < \eta_{jet} < 2.5$ by requiring a jet of transverse energy $E_T^{jet} > 5$ GeV containing an isolated track of transverse momentum $P_T^{track} > 5$ GeV. The final identification of hadronic tau decays is based on a probability density estimation (PDE) method [13, 14]. In the PDE method, a discriminant

$$\mathcal{D} = \frac{\rho_{sig}\left(\vec{x}\right)}{\rho_{sig}\left(\vec{x}\right) + \rho_{bg}\left(\vec{x}\right)}$$

is defined, based on the densities ρ_{sig} of tau–jets and ρ_{bg} of hadronic jets in a six-dimensional space, which is spanned by selected jet-shape observables that are sensitive to the difference in collimation and particle multiplicity between tau–jets and hadronic jets. In this six-dimensional space, the signal and background densities at a point $\vec{x}$ are estimated using Monte Carlo simulations of tau–jets on one hand and hadronic jets on the other hand, by sampling (i.e. counting) the number of simulated tau–jets and hadronic jets in a small six-dimensional box centered around $\vec{x}$.

The jet–shape observables used in this analysis are all reconstructed from the energy distribution of the jet in the calorimeter. They correspond to the first and second moments of the energy distribution in direction transverse and parallel to the jet–axis; to the number of subjets within the jet (for a y–cut of $5 \cdot 10^{-4}$) and to its invariant mass [15]. For tau–jets to be identified as such a discriminant $\mathcal{D} > 0.95$ is required.

Background arising from unidentified electrons faking a hadronic jet signature is removed by requiring $f_{em} > 95\%$ and $f_{em} + f_{LT} > 1.6$, where f_{em} is the electromagnetic energy fraction of the jet and f_{LT} denotes the leading track fraction, defined as the ratio between the momentum of the stiffest track within the jet and the total jet energy.

For events passing the final event selection, a missing transverse momentum of $P_T^{miss} > 20$ GeV is required.

In an $e^{\pm}p$ dataset corresponding to an integrated luminosity of 130 pb^{-1}, 3 events are selected, while only $0.40^{+0.12}_{-0.13}$ are expected from all SM processes. 2 of the 3 events are selected in the region $P_T^X > 25$ GeV (*cf.* figure 3), in which the excess of lepton+P_T^{miss} events is observed in the H1 data, exceeding a SM expectation of 0.20 ± 0.05 events (49% of which are expected from SM $W \to \tau\nu$ decays).

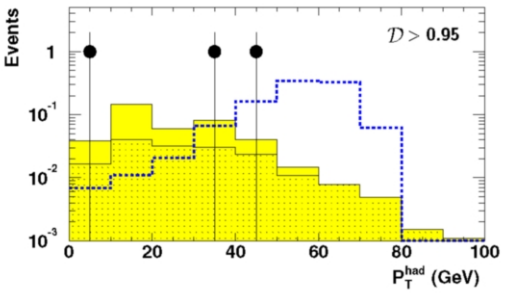

Figure 3. Distribution of the hadronic transverse momentum in the $\tau + P_T^{miss}$ events selected in the ZEUS $e^{\pm}p$ data (points), compared to the SM expectation (solid histogram). The contribution from W boson decays is indicated by the hatched histogram. Also shown in the figure (dashed line) is the hadronic transverse momentum spectrum that might be observed if a signal for new physics (in this example single top quarks produced by flavor–changing neutral current interactions [11]) were present in the ZEUS data.

A review of the H1 and ZEUS results for events containing isolated electrons, muons or tau leptons and large missing transverse momentum has recently been published [16].

In summary, a fluctuation of $\tau + P_T^{miss}$ events over the SM expectation is observed by both H1 and ZEUS in the region of large hadronic transverse momenta P_T^X. In the complementary $e + P_T^{miss}$ and $\mu + P_T^{miss}$ channels, H1 observes an excess of events at high P_T^X in e^+p collisions only. The event yield observed by H1 in e^-p collisions is in good agreement with the SM. ZEUS, on the other hand, sees no indication for an excess in the same channels, neither in e^-p nor in e^+p collisions.

5. Search for doubly charged Higgs Bosons

Doubly charged Higgs bosons arise in models in which the SM Higgs sector is extended by one or more triplet(s) with non–zero hypercharge [17–19]. The Higgs triplet(s) may couple to charged leptons, to other Higgs and to gauge bosons via Yukawa couplings that are in general not related to the fermion masses. Couplings to neutrinos and to quarks are not possible, due to charge conservation.

The H^{++} can be produced at HERA if it has a non–zero coupling (h_{ee}, $h_{e\mu}$ or $h_{e\tau}$) to the electron. Decays to ee, $e\mu$ and $e\tau$ are searched for by H1 and no evidence for such signal is found [20]. Here, the search for production and decay of doubly charged Higgs bosons via the $h_{e\tau}$ coupling is presented in more detail.

$H^{++} \to e\tau$ decays are searched for in a combination of three channels, covering the decays of the tau lepton into an electron ($e + e$ channel), a muon ($e+\mu$ channel) or into a collimated hadronic jet (e+jet channel).

Electrons are required to have a transverse momentum above 5 GeV and to be within the angular range $20^\circ < \theta_e < 140^\circ$ (120° in the $e + \mu$ channel).

Muons are required to have a transverse momentum $P_T^\mu > 5$ GeV and to be within the angular range $20^\circ < \theta_\mu < 140^\circ$.

Hadronic tau decays are selected in the angular range $20^\circ < \theta_{jet} < 140^\circ$ by requiring a jet that contains at least one track of $P_T^{track} > 5$ GeV and no further tracks within a distance of $0.15 < R < 1.5$ around the jet–axis (tracks closer than 0.15 to the jet–axis are interpreted as resulting from three–prong tau decays).

In each channel, at least one electron, muon, or tau–jet with a transverse momentum above 10 GeV is required, in order to insure a high trigger efficiency ($> 95\%$). The charges of the electrons, muons and tau–jets are required to be positive, as expected for leptons produced in H^{++} decays. For events selected in the $e+e$ and e+jet channels, a significant missing transverse momentum ($P_T^{miss} > 8$ GeV in the $e + e$ channel and $P_T^{miss} > 11$ GeV in the e jet channel) is required, indicating the presence of undetected momentum in the final state, resulting from the neutrinos produced in the tau decays. A few more selection criteria are applied, to reduce the contributions from specific background processes. Details of the full event selection can be found in [22].

In the combination of the $e+e$, $e+\mu$ and e+jet channels, the efficiency to select $H^{++} \to e\tau$ signal events amounts to about 25%.

In an e^+p dataset corresponding to an integrated luminosity of 88 pb^{-1}, 1 event is selected in the combination of the three analyzed channels, in agreement with an expectation of 2.07 ± 0.54 arising from SM (background) processes. As no evidence for the production of H^{++} bosons is observed, limits on the mass M_H and on the coupling $h_{e\tau}$ are set [20], which extend the parameter space excluded by H^{++} searches at LEP [21] by the amount shown in figure 4.

6. Search for Lepton Flavor Violation

Within the SM, lepton flavor is conserved individually for each lepton generation in all interactions, in agreement with experimental observations. From a theoretical point of view, the conservation of generation–wise lepton flavor is not mandatory, however, as there is no gauge symmetry that demands it. The observation of lepton flavor violating processes would be a clear indication of physics beyond the SM.

In ep collisions at HERA, lepton flavor violation (LFV) may be observed via a change in lep-

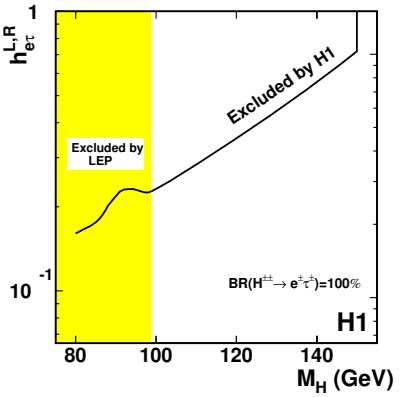

Figure 4. Mass dependent upper limit (at the 95% confidence level) on the coupling $h_{e\tau}$ assuming that the H^{++} decays solely via $H^{++} \to e\tau$. The region above the curve is excluded.

ton flavor of the incoming beam electron into a muon or tau in the final state.

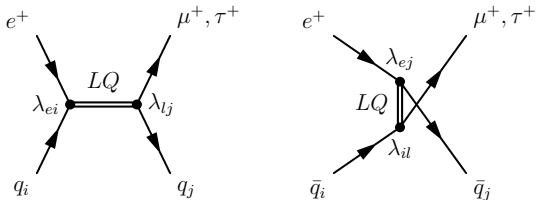

Figure 5. Resonant LQ production in the s–channel with subsequent decay of the produced LQ into a muon or tau lepton (left) and u–channel exchange of a LQ possessing couplings to second or third generation leptons (right).

Lepton flavor violating processes are described by introducing a new particle species, color triplet scalar or vector bosons that carry both lepton and baryon numbers and are hence called "leptoquarks". In the leptoquark (LQ) model, lepton flavor violating processes $ep \to \mu X$ and $ep \to \tau X$ at HERA are described by the two Feynman diagrams shown in figure 5. In the figure, λ_{ei} (λ_{ej}) denotes the Yukawa coupling of a leptoquark to a positron and a quark of generation i (j) and λ_{li} (λ_{lj}) denotes the coupling to the same quark and a lepton of generation l (muon or tau). In the following, results of searches for lepton flavor violating processes $ep \to \tau X$, leading to a tau lepton in the final state, are presented.

6.1. H1 Analysis

The H1 search for LFV via $ep \to \tau X$ processes is based on identifying the hadronic decay products of the tau.

Events are selected by requiring two high P_T jets of transverse momenta $P_T^{jet1} > 25$ GeV and $P_T^{jet2} > 15$ GeV (the higher P_T jet is interpreted as the one resulting from hadronization of the quark and the the lower P_T one as resulting from the tau decay) within the angular range $7^\circ < \theta_{jet1,jet2} < 145^\circ$. In order to reduce the background from unidentified beam electrons faking the signature of a hadronic tau decay, the ratio f_{em} of energy deposited in the electromagnetic calorimeter to the total energy of the jet, deposited in either the electromagnetic and or the hadronic calorimeter, is required to be less than 95% for both jets. The background from hadronic jets is reduced by requiring a jet radius $R_{jet} < 0.12$ (defined in section 4.1), an invariant mass $M_{jet} < 7$ GeV (reconstructed from energy deposits in the calorimeter) and $1 \leq N_{tracks} \leq 3$ tracks within the jet, all within a narrow cone of radius 0.12 around the jet–axis.

For the selected events, a large missing transverse momentum, $P_T^{miss} > 20$ GeV is required, indicating the presence of undetected momentum caused by the tau neutrino. The missing transverse momentum vector is required to line up within $\left|\phi^{jet} - \phi^{miss}\right| < 30^\circ$ with the visible tau decay products in the transverse plane. The efficiency of these selection criteria ranges from about 10% to 30%, depending on the LQ mass and type [3].

In an e^+p dataset corresponding to an integrated luminosity of 66 pb^{-1}, 1 event is selected, in agreement with an expectation of 0.56 ± 0.16 events from SM (background) processes. As no evidence for an observation of LFV is found, lim-

[3]The efficiency depends on the LQ type via the spin of the LQ, as a different LQ spin results in different angular distribution and hence a different geometric acceptance of the selection criteria.

its on the couplings and masses of leptoquarks are set [23].

6.2. ZEUS Analysis

In the analysis performed by the ZEUS collaboration, $ep \to \tau X$ events are selected in a combination of electronic, muonic and hadronic decay modes of the produced tau lepton.

Electrons are required to have an energy $E_e > 20$ GeV and be within the angular range $8° < \theta_e < 125°$.

Muons are selected in the angular range $8° < \theta_\mu < 164°$ by requiring the presence of either an isolated track with a transverse momentum > 5 GeV in the cylindrical drift chamber that is matched to an energy deposit compatible with a minimum ionizing particle signature in the calorimeter or a track reconstructed in the forward muon detector.

Hadronic tau decays are identified in the angular range $15° < \theta_{jet} < 164°$ by a cut $D > 0.90$ on the discriminant described in section 4.2 (using the same six jet–shape observables as those used in the ZEUS $\tau + P_T^{miss}$ analysis). Background from unidentified beam electrons is removed by requiring $f_{em} > 95\%$ and $f_{em} + f_{LT} > 1.6$ (*cf.* section 4.2).

For the selected events, a missing transverse momentum $P_T^{miss} > 15$ GeV (> 20 GeV for events selected in the muonic decay mode) lined up within $\left|\phi^{e,\mu,jet} - \phi^{miss}\right| < 20°$ with the visible tau decay products in the transverse plane is required. Remaining background contributions are reduced by a few more selection criteria, the details of which can be found in [24].

In an $e^{\pm}p$ dataset corresponding to an integrated luminosity of 130 pb^{-1}, 0 events are selected in the combination of leptonic and hadronic decay modes, compatible with a SM (background) expectation of 2.3 ± 0.5 events. In the absence of a signal, limits on the masses and couplings of the leptoquarks are set.

Some of the ZEUS limits actually represent the most stringent bounds on leptoquark masses and couplings available to date, improving the limits [25] obtained from searches for rare tau lepton, Kaon and B meson decays by up to a factor four [24]. As an example, ZEUS limits on leptoquarks of masses near the HERA kinematic limit, obtained from the search for lepton flavor violating processes $ep \to \tau X$, are compared with the parameter space excluded by low energy experiments in figure 6.

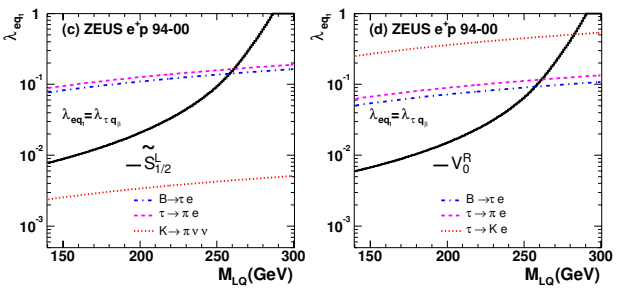

Figure 6. Mass dependent upper limits (at the 95% C. L.) on the coupling $\lambda_{\tau q}$ for scalar (left) and vector (right) leptoquarks obtained by the ZEUS search for LFV compared to the parameter space excluded by low energy experiments.

7. Summary

Four different types of analyses investigating the production of tau leptons in ep collisions at HERA have been presented. The results of the H1 and ZEUS $\tau^+\tau^-$ analyses agree well with the SM predictions. No evidence for doubly charged Higgs bosons or lepton flavor violation has been found.

In the analysis of $\tau + P_T^{miss}$ events a fluctuation of events over the SM expectation is observed in the region of large hadronic transverse momenta P_T^X. However, provided the limited statistics of the available data samples, the results of the H1 and ZEUS analyses do not allow for final conclusions yet.

It will therefore be very interesting to see how the excess of $e + P_T^{miss}$, $\mu + P_T^{miss}$ and $\tau + P_T^{miss}$ events develops in the future. The datasets analyzed in the lepton+P_T^{miss} analyses at HERA so far correspond to integrated luminosities of 341 pb^{-1} (e+P_T^{miss} and μ+P_T^{miss}, H1), 278 pb^{-1} ($\tau + P_T^{miss}$, H1), 250 pb^{-1} ($e + P_T^{miss}$ and $\mu + P_T^{miss}$, ZEUS) and 130 pb^{-1} ($\tau + P_T^{miss}$, ZEUS). By the time of the HERA shutdown scheduled

for end of June next year, each experiment is expected to have collected in total $\sim$500 pb^{-1} of data. The datasets available for analyses will then be about twice as large as the datasets that have been analyzed to date.

REFERENCES

1. Grape 1.1, T. Abe, Comput. Phys. Commun. 136 (2001) 126 [hep-ph/0012029].
2. K. P. Diener, C. Schwanenberger and M. Spira, Eur. Phys. J. C 25 (2002) 405 [hep-ph/0203269].
3. I. Abt et al. [H1 Collaboration], Nucl. Inst. Meth. A 386 (1997) 310 and 348.
4. U. Holm (ed.) [ZEUS Collaboration], The ZEUS detector, (unpublished), DESY (1993), available at http://www-zeus.desy.de/bluebook/bluebook.html.
5. A. Aktas et al. [H1 Collaboration], Eur. Phys. J. C 31 (2003) 17 [hep-ex/0307015].
6. A. Aktas et al. [H1 Collaboration], Phys. Lett. B 583 (2004) 28 [hep-ex/0311015]; H1 Collaboration, Multi–lepton events at HERA, contributed paper to Int. Conf. on High Energy Physics, Jul 26-Aug 2, 2006, Moscow.
7. ZEUS Collaboration, Int. Conf. on High Energy Physics, Aug 12-22, 2004, Beijing, Abstract 230, Parallel Session 12; ZEUS Collaboration, Study of Multi-lepton Production with the ZEUS detector at HERA, contributed paper to Int. Conf. on High Energy Physics, Jul 26-Aug 2, 2006, Moscow.
8. C. Veelken, PhD thesis, University of Liverpool, 2006, available at http://www-h1.desy.de/publications/thesis_list.html.
9. A. Aktas et al. [H1 Collaboration], submitted to Eur. Phys. J. C [hep-ex/0604022].
10. T. Ahmed et al. [H1 Collaboration], DESY preprint 94-248 (1994); C. Adloff et al. [H1 Collaboration], Eur. Phys. J. C 5 (1998) 575 [hep-ex/9806009]; V. Andreev et al. [H1 Collaboration], Phys. Lett. B 561 (2003) 241 [hep-ex/0301030].
11. H. Fritzsch and D. Holtmannspotter, Phys. Lett. B 457 (1999) 186 [hep-ph/9901411]; see also A. Aktas et al. [H1 Collaboration], Eur. Phys. J. C 33 (2004) 9 [hep-ex/0310032] and S. Chekanov et al. [ZEUS Collaboration], Phys. Lett. B 559 (2003) 153 [hep-ex/0302010].
12. H1 Collaboration, Search for Events with Isolated Tau-Leptons and Missing Transverse Momentum at HERA, contributed paper to Int. Workshop on Deep Inelastic Scattering, Apr 20-24, 2006, Tsukuba.
13. T. Carli and B. Koblitz, Nucl. Inst. Meth. A 501 (2003) 576.
14. R. O. Duda, P. E. Hart and D. G. Stork, Pattern Classification, Wiley, 2003.
15. C. N. Nguyen, Diploma thesis, Univ. Hamburg (2002) [DESY-THESIS-2002-024].
16. J. Ferrando, Mod. Phys. Lett. A 21 (2006) 1901.
17. G. B. Gelmini and M. Roncadelli, Phys. Lett. B 99 (1981) 411.
18. J. C. Pati and A. Salam, Phys. Rev. D 10 (1974) 275; R. E. Marshak and R. N. Mohapatra, Phys. Lett. B 91 (1980) 222.
19. R. N. Mohapatra and G. Senjanovic, Phys. Rev. Lett. 44 (1980) 412.
20. A. Aktas et al. [H1 Collaboration], Phys. Lett. B 638 (2006) 432.
21. P. Achard et al. [L3 Collaboration], Phys. Lett. B 576 (2003) 18 [hep-ex/0309076]; G. Abbiendi et al. [OPAL Collaboration], Phys. Lett. B 526 (2002) 221 [hep-ex/0111059].
22. S. Baumgartner, PhD thesis, ETH Zürich (2005) [ETH-16125], available at http://www-h1.desy.de/publications/thesis_list.html.
23. H1 Collaboration, Int. Conf. on High Energy Physics, Aug 12-22, 2004, Beijing, Abstract 766, Parallel Session 12.
24. S. Chekanov et al. [ZEUS Collaboration], Eur. Phys. J. C 44 (2005) 463 [hep-ex/0501070].
25. E. Gabrielle, Phys. Rev. D 62 (2000) 55009 [hep-ph/9911539].